ANALYSIS OF STABILITY AND PERFORMANCE OF AN OIL WELL DRILLING OPERATION SUBJECT TO STICK-SLIP USING NON-COLLOCATED LINEAR VELOCITY CONTROL

Leopoldo M. Manzatto, lmanzatto@sc.usp.br
Marcelo A. Trindade, trindade@sc.usp.br
Department of Mechanical Engineering, São Carlos School of Engineering, University of São Paulo, Av. Trabalhador São-Carlense, 400, São Carlos-SP, 13566-590, Brazil

Abstract. *Drilling operations for oil and gas wells requires the control of a very flexible structure subjected to complex and nonlinear boundary conditions. One of the most important causes of failure in drill-strings and drill-bits is the stick-slip phenomenon occurring at drill-bit/formation interface. Previous results confirm that a standard proportional-integral velocity control driving system may lead to a fluctuating drill-bit angular velocity. This work presents a parametric analysis of the dynamic response of a simplified model for a drilling system composed of driving rotary table, drillstring and bottom-hole-assembly. The drill-bit-formation interaction is modeled using a nonlinear non-regularized dry friction model. The main objective is to show that depending on the operation conditions, weight-on-bit and target angular velocity, there exist well-defined stability regions on the plane formed by the proportional and integral control parameters in which the self-excited torsional vibrations (and oscillatory angular velocities) induced by the stick-slip phenomenon may be reduced. The behaviors of these stability regions in terms of varying operation conditions are analyzed. The effect of the control parameters and operation conditions on some performance and failure criteria, such as average rate-of-penetration, driving torque and power required, maximum drill-bit angular velocity, and maximum shear stress in the drillstring, is also analyzed.*

Keywords: *Oil well drilling; stick-slip phenomenon; drillstring dynamics; linear non-collocated velocity control*

1. INTRODUCTION

According to Jansen and van den Steen (1995), the drilling of oil wells involves the opening of wells in rock formations with diameters of about 10 to 85 cm and depths from 0 to 5000 meters for the extraction of oil and gas. The commonly used drilling mechanism is composed of one or more relatively complex coupled systems (electrical, mechanical, hydraulic, etc). During the drilling process, axial, torsional and lateral vibrations, or combinations of these, are generated leading to one of the main problems on the oil well drilling process (Schlumberger, 2006). According to Placido, Santos and Galeano (2002), stick-slip due to torsional vibrations is one of the main phenomena causing failures in the drilling process. Stick-slip is characterized by the stop of the drill bit (bottom) while the rotary table (top) keeps spinning and delivering power, so that, it increases the torsional strain energy that are stored in the drillstring column and, therefore, the torque applied to drill-bit, until it overcomes the friction resistance between the bit and the ground starting to drill again, but with speeds much higher than the target one. In practical measurements made by Placido, Santos and Galeano (2002), the stick-slip is observed by strong oscillations in the drilling speed. This oscillation is self-excited becoming regular and stable once the mode starts and is reduced if the speed is increased (Placido, Santos and Galeano, 2002; Trindade and Sampaio, 2005). The frequency of these oscillations is usually somewhat below the first natural frequency of torsional vibration in the range of 0.05 to 0.5 Hz (Jansen and van den Steen, 1995).

Despite the fact that the propagation of torsional disturbances is governed by linear wave equations, the interaction between drill-bit and rock formation presents a highly non-linear behavior which can be a cause of non-uniform penetration (Spanos et al., 1995, Tucker and Wang, 2003). The stick-slip induces bit torsional relaxation associated with the frictional torque that is function of angular velocity and weight on bit (WOB). Richard and Detournay (2000) have studied the self-excited response of such systems using a discrete model with two degrees of freedom (dof) to demonstrate that the linear coupling between the normal and tangential modes are sufficient to generate a stick-slip. Ritto, Soize and Sampaio (2009) also studied the nonlinear interaction between bit and rock formation but using a stochastic model for the main forces acting on the system.

Jansen and van den Steen (1993) assumed a simplified friction model that captures the essence of the non-linear effect that is sufficient to perform linear analyses. Tucker and Wang (1999b) used a continuum approach for the column combined to a friction model between bit and rock formation that is a function of relative motion. Once stick-slip induced vibrations have a fundamental role in the drilling process, several different techniques have been proposed along the years to control this phenomena. They can be summarized in the following categories: active damping (Jansen and van den Steen, 1993), torque rectification (Tucker and Wang, 1999a), soft-torque (Tucker and Wang, 1999a; Tucker and Wang, 2003), proportional-integral (PI) rotary speed control (Christoforou and Yigit, 2003; Trindade and Sampaio, 2005) and weight on bit dynamic variation (Lopez and Suarez, 2004).

Several theoretical and numerical studies were carried out to identify and minimize drilling problems due to stick-slip phenomenon. For that, variations of simplified dynamic models were considered to represent the drilling

mechanism composed of the rotary table, drillstring and BHA (Bottom-Hole Assembly, that include the drill bit). They can be classified in models with distributed parameters as those studied by Tucker and Wang (1999b), Trindade, Wolter and Sampaio (2005), Trindade and Sampaio (2005) and Ritto, Soize and Sampaio (2009), and with discrete parameters as Richard and Detournay (2000), Christoforou and Yigit (2003), Richard, Germay and Detournay (2004) and Lopez and Suarez (2004). These models could also be classified by their quality of approximation and complexity depending on the number of resulting dof. Other relevant studies, such as the one of Elsayed, Dareing and Vonderheide (1997), analyzed the effect of torsional vibrations on the system stability through a frequency analysis.

Based on this literature review, one can conclude that the reduction of torsional vibrations and stick-slip phenomenon in the drilling process remains a challenge. Hence, this work presents preliminary results of a parametric analysis based on operating conditions and control parameters using linear velocity control combined to a coupled structural model and accounting for the non-linear interaction between drill-bit and rock formation. The main objective of this work is to identify ranges of operating conditions and control parameters that may lead to a stable and satisfactory drilling process.

2. DRILLING MECHANISM COUPLED MODEL

A two dof dynamic model composed of a BHA connected to a rotary table by a flexible drillstring, as represented in Fig. 1, is considered. The drill-bit has moment of inertia J_b, angular velocity ω_b and angular displacement θ_b. The rotary table has moment of inertia $J_{m,}$, angular velocity ω_m and angular displacement θ_m. The drillstring is approximated by a cylinder of length L, moment of inertia J_c and effective stiffness coefficient k_θ.

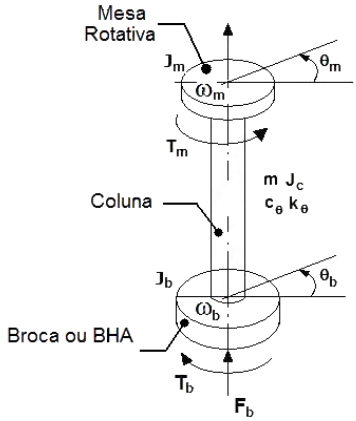

Figure 1 – Two dof model for the drilling mechanism.

2.1. Structural model

The equations of motion for the model can be written as

$$\left(J_m + \frac{1}{2}J_c\right)\ddot{\theta}_m + c_\theta(\omega_m - \omega_b) + k_\theta(\theta_m - \theta_b) = T_m, \tag{1}$$

$$\left(J_b + \frac{1}{2}J_c\right)\ddot{\theta}_b + c_\theta(\omega_b - \omega_m) + k_\theta(\theta_b - \theta_m) = -T_b. \tag{2}$$

The drillstring moment of inertia has significant influence, therefore, it was divided into two parts, half being added to the moments of inertia of the drill-bit assembly and the rotary table. The equivalent damping coefficient c_θ was defined a posteriori during the numerical simulations. The stiffness coefficient k_θ is calculated based on the shear modulus G, length L and second moment of cross-section area I_c of the drillstring, considering a homogeneous cylinder with is external and internal diameters D_c and d_c, such that

$$k_\theta = \frac{G\, I_c}{L}, \tag{3}$$

$$I_c = \left(\frac{\pi}{32}\right)\left[{D_c}^4 - {d_c}^4\right]. \tag{4}$$

2.2. Interaction between drill-bit and rock formation

The most important aspect of the drilling process is the contact between drill-bit and rock formation. The bit is subjected to angular velocity ω_b and axial force F_b (WOB) and torque T_b on the interface with rock formation. The torque transmitted by the drillstring is denoted T. Figure 2 presents the schematic of the forces acing on the process.

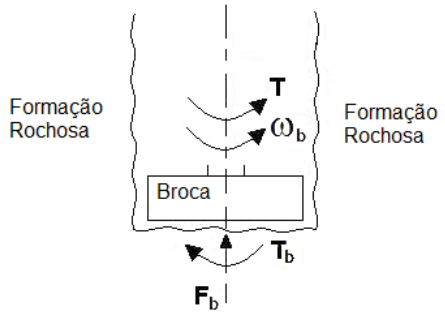

Figure 2 – Schematics of drill-bit and rock formation interface.

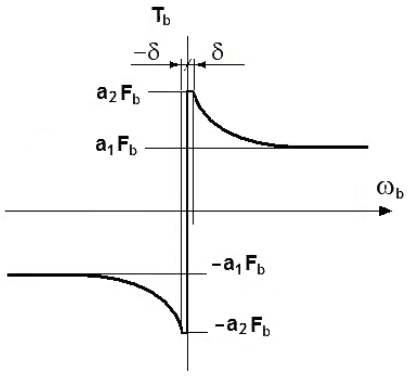

Figure 3 – Friction model.

Previous studies (Richard and Detournay, 2000; Richard, Germay and Detournay, 2004) show that, in fact, based on drilling characteristics and conditions, the stick-slip phenomenon can be represented using a dry friction model. Based on that, there are three basic conditions that can be set to represent the torque induced between drill-bit and rock formation:

$$T_b = T, \qquad |\omega_b| \leq \delta \; e \; |T| \leq a_2 F_b \, ; \tag{4}$$

$$T_b = a_2 F_b \; sign\,(T), \qquad |\omega_b| \leq \delta \; e \; |T| > a_2 F_b \, ; \tag{5}$$

$$T_b = \left[a_1 + (a_2 - a_1) e^{-\beta |\omega_b|}\right] F_b sign(\omega_b), \quad |\omega_b| > \delta. \tag{6}$$

Equation (6) defines the condition in which the drilling operation is in stick phase, its angular velocity ω_b is approximately zero and the torque applied does not exceed the maximum permissible torque between drill-bit and rock formation interface. In the equation (7), the drill-bit begins to enter the slip phase and therefore restart drilling. In this case, the applied torque exceeds the maximum permissible torque, and the drill bit from this point has angular acceleration. Equation (8) establishes the behavior of the torque on the drill-bit when in motion that is function of its angular velocity. The last equation does also include the intermediate phase transition between the stick and slip conditions. Figure 3 graphically represents the friction model considered for torque on the bit.

2.3. Curve fit of friction model parameters

The equivalent friction model parameters a_1, a_2 and β are defined in terms of the drilling operation and the rock formation conditions. They represent, respectively, dynamic and static equivalent friction coefficient and exponential decay coefficient adjusted manually relative to the reference (Trindade and Sampaio, 2005).

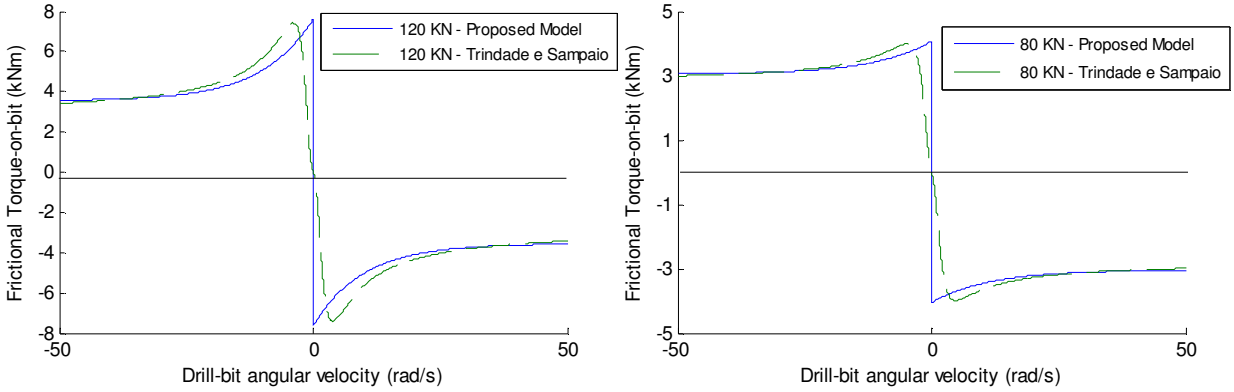

Figure 4 – Comparison between the friction torque versus drill-bit angular velocity curve evaluated with the proposed model and the reference one for two weights on bit: (a) 120 kN and (b) 80 kN.

The proposed model parameters for the two loading conditions (weights on bit of 120 kN and 80 kN) were found by manually curve fitting the corresponding friction torque versus drill-bit angular velocity curves to those obtained using the reference model (Trindade and Sampaio, 2005). The curves are shown in Fig. 4. The model parameters were found to be: $a_1 = 0.7$, $a_2 = 1.5$ and $\beta = 0.10$ for 120 kN, and $a_1 = 0.9$, $a_2 = 1.2$ and $\beta = 0.09$ for 80 kN. In order to study

different weight on bit conditions, a linear interpolation of parameters was done to adjust the model. The parameters for this model are presented in Table 1 for five drilling loading conditions from 80 to 160 kN. It is important to emphasize, however, a fundamental difference between the proposed model and the reference one to adjust the parameters. In the proposed model, the torque on bit on the stick phase depends on the static equilibrium of the structure, while in the reference model a regularization function is used. Therefore, the results are quite different for small angular velocities.

Table 1 – Fitted friction model parameters for loading conditions (WOB) from 80 to 160 kN.

Weight on bit (kN)	a_1	a_2	β
80	0.900	1.200	0.090
100	0.800	1.350	0.095
120	0.700	1.500	0.100
140	0.625	1.575	0.100
160	0.550	1.650	0.100

2.4. Control strategy description

The proposed control strategy is a traditional technique, which consists on a control torque that is proportional-integral (PI) to the angular velocity. Due to the nature of the drilling operation, it is not possible to measure the angular velocity and apply the control torque to the drill-bit but, instead, the angular velocity of the rotary table is measured and the control torque is applied to the rotary table. This is denoted here as a non-colocalized control technique in the sense that the control of angular velocity at the rotary table does not guarantee a satisfactory control of the angular velocity at the drill-bit. Indeed, the torque applied to the rotary table is transmitted to the drill-bit through the flexible drillstring (Trindade and Sampaio, 2005; Tucker and Wang, 1999a). The control torque is a function of the target and real angular velocities and angular positions according to

$$T_m = k_p(\Omega - \omega_{\mathrm{m}}) + k_i(\Theta - \theta_{\mathrm{m}}), \tag{7}$$

where θ_m is the real angular position of the rotary table and ω_m its real angular velocity. Θ and Ω are the corresponding target values for the drill-bit angular position and angular velocity. Hence, the desired objective of the control torque would be to minimize the difference between actual and target angular velocities in the drill-bit.

3. PARAMETRIC ANALYSIS FOR A TYPICAL DRILLING MECHANISM

Based on the proposed simplified model, represented in Fig. 1, numerical simulations were performed using typical drilling mechanism parameters adapted from the works of Trindade and Sampaio (2005) and Tucker and Wang (2003). These are: shear modulus $G = 79.6$ GPa, length $L = 3000$ m, external diameter $D_c = 0.1270$ m, internal diameter $d_c = 0.1086$ m, and moment of inertia $J_c = 285$ kg m^2 for the drillstring; moment of inertia $J_m = 500$ kg m^2 for the rotary table; and moment of inertia $J_b = 394$ kg m^2 for the BHA (bottom-hole assembly including drill-bit). The equivalent viscous damping coefficient was assumed as $c_\theta = 10^{-6}$ Nm^{-1}s^{-1}. These parameters yield an open-loop natural frequency of 0.165 Hz for the drilling mechanism.

Based on current drilling studies, the operating conditions will be set in terms of desired weight-on-bit and drill-bit angular velocity. The studies used as reference to the present work (Trindade and Sampaio, 2005; Tucker and Wang, 2003) assumed a weight-on-bit of 120 kN and a target drill-bit angular velocity of 100 rpm (10.47 rad/s). Here, in addition to that one, other operating conditions will be considered. For that, three values are considered for the target drill-bit angular velocity, 80, 100 and 120 rpm, and for the weight-on-bit, 80, 100 and 120 kN. It is well known that the stick-slip phenomenon is enhanced for low angular velocities and high weights-on-bit. Therefore, it is expected that the worst condition should be 120 kN and 80 rpm and the more relieved condition should be 80 kN and 120 rpm.

A first approach to understanding the effect of control parameters was to analyze the time-domain response of the system when the control parameters are varied relative to the case studied in (Trindade and Sampaio, 2005; Tucker and Wang, 2003). From the control law, it is possible to associate the integral component (proportional to the angular position) to an increase in the equivalent stiffness of the system and, thus, of its natural frequency; whereas the proportional component (proportional to the angular velocity) relates to an increase in the equivalent damping of the system. Figures 5, 6 and 7 present the time-domain response of the system when using the control parameters considered in the reference case (k_p=200 Nm and k_i=100 Nm, Fig. 5) and when the integral gain k_i is increased to 200 Nm (Fig. 6) and decreased to 50 Nm (Fig. 7). It can be noticed that when the integral gain is increased the frequency of angular velocity oscillations is also increased (Fig. 6) and vice-versa (Fig.7). While a decrease in the integral gain seems to solve the stick-slip problem, since the response converges to a steady state with no stick-slip (Fig. 7), it should be noticed that this also yields a relatively long stick phase (the drill-bit remains more than 15 seconds in stick phase) which may lead to drillstring failure.

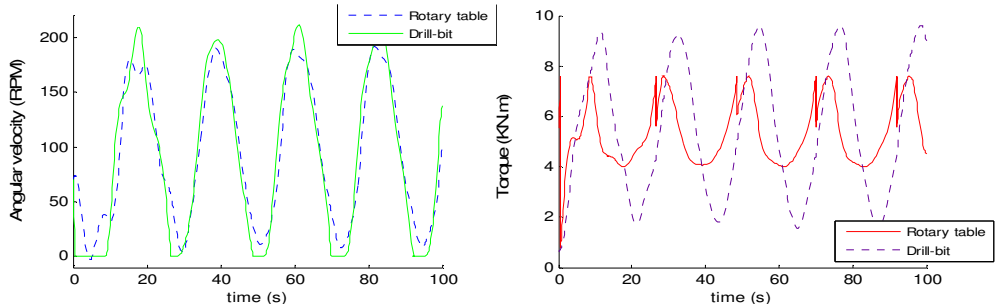

Figure 5 – Time response for 120 kN and 100 rpm drilling conditions with $k_i = 100$ Nm and $k_p = 200$ Nms.

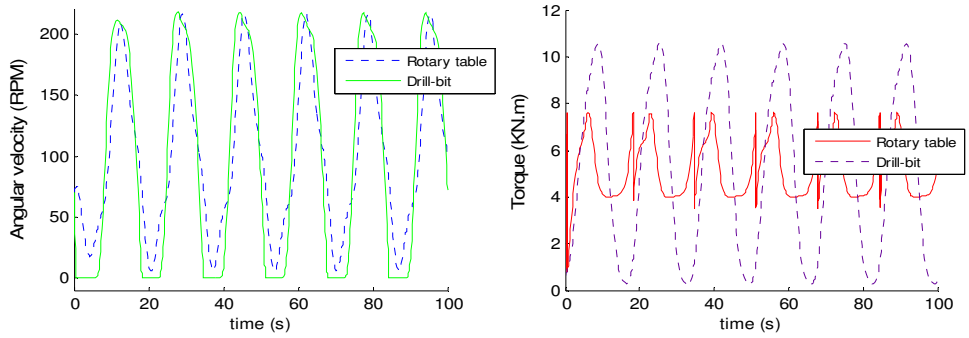

Figure 6 – Time response for 120 kN and 100 rpm drilling conditions with $k_i = 200$ Nm and $k_p = 200$ Nms.

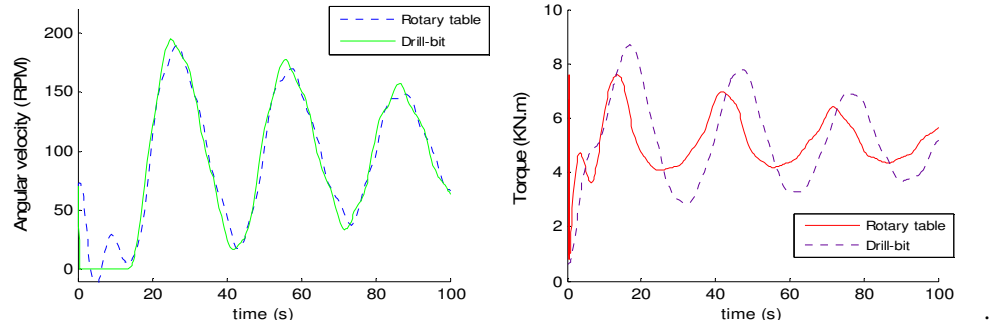

Figure 7 – Time response for 120 kN and 100 rpm drilling conditions with $k_i = 50$ Nm and $k_p = 200$ Nms.

This analysis indicates that the control parameters have significant influence and that, for a given operating condition, the stick-slip could be minimized by an adequate choice of control parameters. Therefore, a parametric analysis was performed to evaluate the drilling performance when the control parameters are varied. Based on preliminary analyses, 32 values were considered for the proportional (k_p) and integral (k_i) control parameters in the ranges $k_p \in [1; 1000]$ Nms and $k_i \in [1; 500]$ Nm. The resulting equations of motion were integrated from 0 to 100 seconds using MATLAB® Runge-Kutta fourth and fifth order ordinary differential equations integrator (ODE45). A value of 0.001 was considered for the null angular velocity threshold δ used in the friction model (Eqs. 5-7).

In order to simplify the parametric analysis, some relevant metrics were considered to qualify the time response of the system, such as the average deviation of drill-bit angular velocity, average deviation of rate-of-penetration (ROP), maximum shear stress in the drillstring, maximum deviation of drill-bit angular velocity, maximum torque on drill-bit and maximum power at rotary table. The first metric indicates the overall stability of the system, the second, the overall performance, the third, fourth and fifth metrics relate to main causes of process failure (drillstring and drill-bit failures), and the last metric measures the control effort. Due to space restrictions, only the first two of these metrics are presented in this work.

3.1. Average deviation of drill-bit angular velocity

This metric evaluates the average deviation of the drill-bit angular velocity with respect to the target angular velocity and, thus, measures if and to what extent the angular velocity is oscillatory indicating the occurrence of stick-slip phenomenon. The metric is based on the actual drill-bit angular velocity ω_b and target angular velocity Ω, such that

$$J_1 = \int_{t_i}^{t_f} \frac{|\omega_b - \Omega|}{\Omega} dt. \tag{8}$$

Figure 8 shows the behavior of the J_1 metric for the different values for control parameters considering the following target drilling conditions: weight-on-bit 100 kN and drill-bit angular velocity 100 rpm. It is possible to observe that there is a region (region 2 in Fig. 8) in which the angular velocity deviation is relatively small (~10%), indicating less stick-slip, while in other regions it may reach high values (up to 90%). In the region 1, low values are considered for the integral control parameter k_i (less than 50 Nm) leading to angular velocity deviations between 17% and 50%, indicating that the velocity control system is not very effective. In the region 3, relatively low values are considered for the proportional control parameter k_p (less than 400 Nm) leading to high angular velocity deviations between 65% and 89% indicating several numbers of stick-slip occurrences. The region 2 presents significantly smaller angular velocity deviations, between 5% and 11%, indicating a much more effective velocity control but with the cost of higher values for both control parameters.

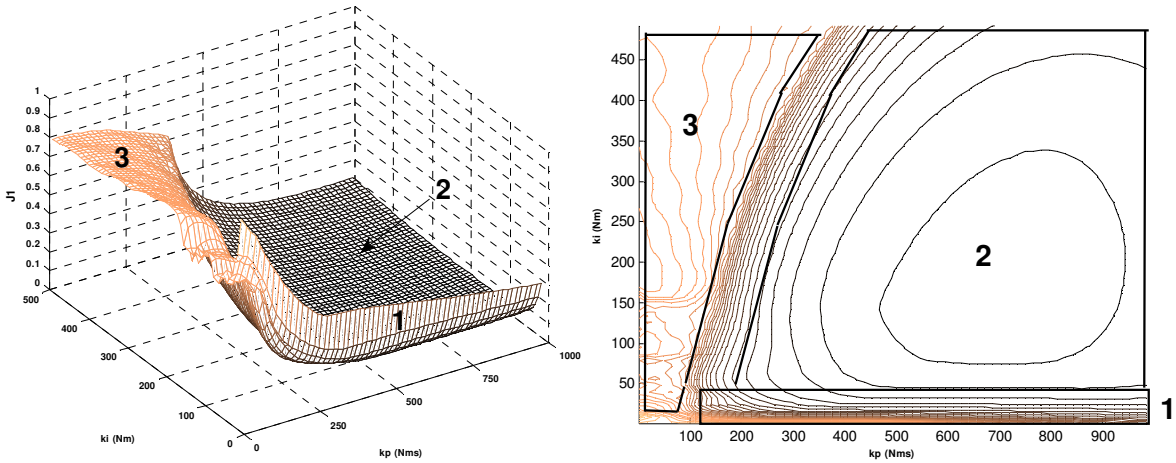

Figure 8 – Average deviation of drill-bit angular velocity for different control parameters.

3.2. Average deviation of rate-of-penetration

Although stability and risk of failure are important factors to be managed in practice, the rate-of-penetration is one of the main criteria to identify the overall performance of the drilling process. It measures the speed of well drilling, in terms of depth of perforated well (in linear meters) over time spent (normally, in hours). A phenomenological expression for the rate-of-penetration was presented by Tucker and Wang (2003) in terms of the weight-on-bit (F_b) and drill-bit angular velocity (ω_b) as

$$\mathrm{ROP}^\mathrm{t} = -c_1 + c_2 F_\mathrm{b}^\mathrm{t} + c_3 \omega_\mathrm{b}^\mathrm{t}, \tag{9}$$

where the superscript t stands for target values. The constants in Eq.(10) are fitted to experimental observation and, thus, represent particular drilling conditions, drill-bit design and rock formation characteristics. For the case studied here the following constants were used (Tucker and Wang, 2003): $c_1 = 3.429\ 10^{-3}$ ms^{-1}, $c_2 = 5.672\ 10^{-8}$ mN^{-1}s^{-1}, and $c_3 = 1.374\ 10^{-4}$ mrad^{-1}. Although the target rate-of-penetration ROP^t is completely defined by the target weight-on-bit and target drill-bit angular velocity and, thus, is constant for a given drilling condition, the actual rate-of-penetration is not constant since the drill-bit angular velocity may vary due to stick-slip phenomenon. Therefore, an average rate-of-penetration is evaluated as

$$\mathrm{ROP}^\mathrm{m} = \left[\int_{t_i}^{t_f} (-c_1 + c_2 F_\mathrm{b} + c_3 \omega_\mathrm{b}) dt\right] / (t_f - t_i). \tag{10}$$

Then, the average deviation of rate-of-penetration is defined as the relative difference between the actual and target rates-of-penetration, indicating the overall performance of the drilling process, as

$$J_2 = \frac{\mathrm{ROP}^\mathrm{m} - \mathrm{ROP}^\mathrm{t}}{\mathrm{ROP}^\mathrm{t}}. \tag{11}$$

Figure 9 shows the behavior of this metric for target drilling condition with 100 kN weight-on-bit and 100 rpm drill-bit angular velocity when the control parameters k_p and k_i are varied over the previously defined ranges. As in the previous analysis, three regions with boundaries reasonably well defined can be identified. The region 1, with low integral control gains, contains the cases with higher absolute rate-of-penetration deviations, some of which may present an average rate-of-penetration up to 25% smaller than the target one. In the region 3, which was considered unstable in

the previous analysis, leading to severe oscillations of the angular velocity, the rate-of-penetration deviation is much less affected ranging from 0.1% to 2.3% (smaller than the target ROP). In fact, it can be noticed that there are several cases with better ROP performance in this region than in the stable region (region 2). Indeed, for the region 2, which yields a more stable angular velocity behavior, the average loss in rate-of-penetration, relative to the target one, remains close to 2%.

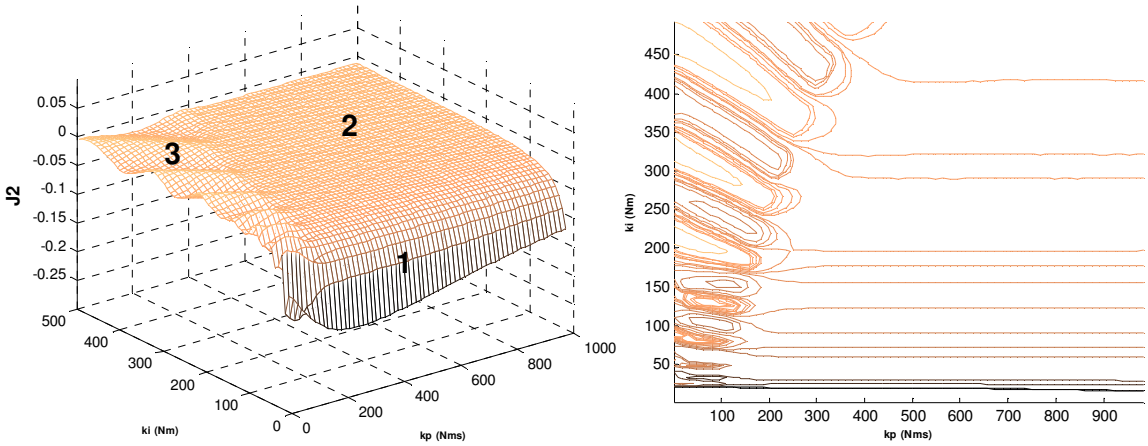

Figure 9 – Average deviation of rate-of-penetration for different control parameters.

4. STRATEGIES TO IMPROVE DRILLING PERFORMANCE

The previous analysis indicates that, for each drilling condition, a set of control parameters can be selected to improve drilling performance. Based on the two criteria presented in the previous section and other important criteria, such as maximum shear stress in the drillstring, maximum deviation of drill-bit angular velocity, maximum torque on drill-bit and maximum power at rotary table, it was found that relatively high values of proportional control gain $600 < k_p < 800$ Nms and relatively low values of integral control gain $50 < k_i < 100$ Nm yield better results. However, the optimal values for the control parameters depend on the weight considered for each one of these criteria and also on the drilling condition.

Instead of finding the optimal control parameters for each drilling condition, it was chosen here to start from the worst drilling condition (highest weight-on-bit, 120 kN, and lowest drill-bit angular velocity, 80 rpm) and search for strategies to improve the overall drilling performance. One strategy would be to adjust the drilling conditions by relieving the weight-on-bit, increasing the drill-bit angular velocity or both. The second strategy would be to modify the control parameters through the kind of analysis presented previously. The third combines the two previous strategies.

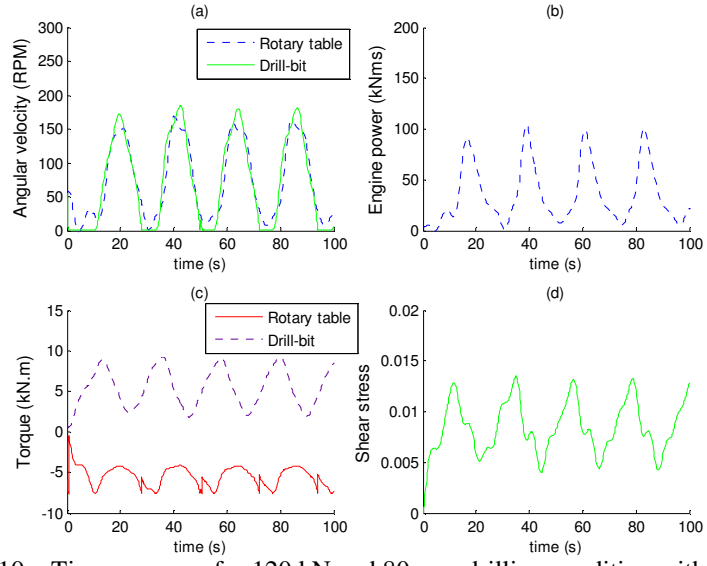

Figure 10 – Time response for 120 kN and 80 rpm drilling condition with control parameters $k_p = 200$ Nms and $k_i = 100$ Nm.

Figure 10 presents the time response of angular velocity and torque, at drill-bit and rotary table, power at rotary table and shear stress in the drillstring, relative to yield stress, for 120 kN and 80 rpm drilling condition with control

parameters $k_p = 200$ Nms and $k_i = 100$ Nm. It can be noticed that stick-slip phenomenon occurs with a period of about 25 seconds, leading to highly oscillatory angular velocity which may reach more than the double of the target one. The other quantities are also oscillatory. This condition presents unnecessary control effort and stress in the drillstring. However, the average rate-of-penetration 15.8 m/h is not much smaller than the target one 16.3 m/h.

4.1. Variation of control parameters

In order to improve the drilling response presented previously, the first strategy would be to modify the control parameters k_p and k_i, according to the parametric analysis presented in Section 3 that suggest higher values for k_p and lower values for k_i. Therefore, first k_p is increased to 500 Nms and k_i is decreased to 50 Nm. The corresponding system response is shown in Fig. 11. It can be noticed that the there is only one initial occurrence of stick-slip and, then, the angular velocity quickly stabilizes, converging to the target one. Similar behavior is observed for other quantities. Maximum power is decreased from 100 kNms, in previous case, to 50 kNms. However, the drill-bit initially remains stopped for about 12 seconds until the stick resistance is exceeded. The average rate-of-penetration for this case is 15.7 m/h, which is a little smaller than the previous one.

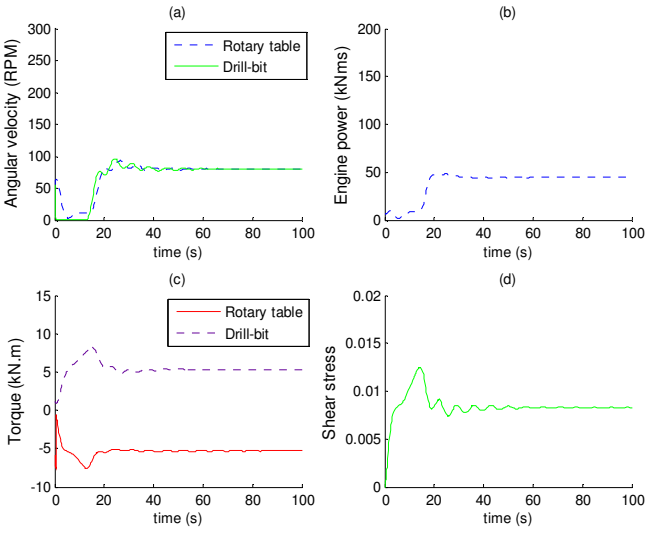

Figure 11 – Time response for 120 kN and 80 rpm with control parameters $k_p = 500$ Nms and $k_i = 50$ Nm.

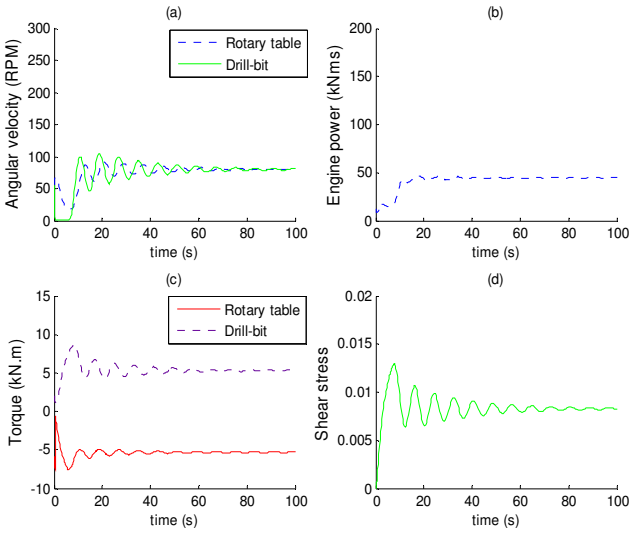

Figure 12 – Time response for 120 kN and 80 rpm with control parameters $k_p = 800$ Nms and $k_i = 100$ Nm.

In a second analysis, the proportional control gain k_p is further increased to 800 Nms and the integral control gain k_i is set to 100 Nm. The response is presented in Fig. 12 where it is shown that the drill-bit starts drilling faster than in the previous case but after that there is more oscillation especially on both angular velocities. The average rate-of-penetration is somewhat increased to 15.9 m/h.

4.2. Variation of drilling conditions

The second strategy to improve drilling performance, often used in the drilling operation, consists in relieving the weight-on-bit and/or increasing the angular velocity whenever stick-slip phenomenon is observed. Increasing the angular velocity from 80 rpm to 120 rpm, the system response is improved with only two stick slip occurrences and a clear convergence tendency (Figure 13). The maximum power required increase to 150 kNms due to angular velocity oscillation but also due to the increase in the target angular velocity and, thus, this may require a redesign of the power drive. The shear stress in the drillstring has wide variation during the first 50 seconds. In terms of average drilling performance, this strategy leads to an average rate-of-penetration of 18.0 m/h (while the target one for such drilling condition would be 18.4 m/h). Besides increasing the angular velocity, it could also be helpful to relieve the weight-on-bit from 120 kN to 100 kN. Indeed, as it can be observed in the resulting time response (Figure 14), there is only one initial occurrence of stick-slip phenomenon followed by a convergent behavior. As expected, all efforts were reduced: the peak power requirement drops to 108 kNms and the shear stress amplitude decreases significantly. However, both target and average rates-of-penetration are reduced to 14.3 m/h and 14.0 m/h, respectively.

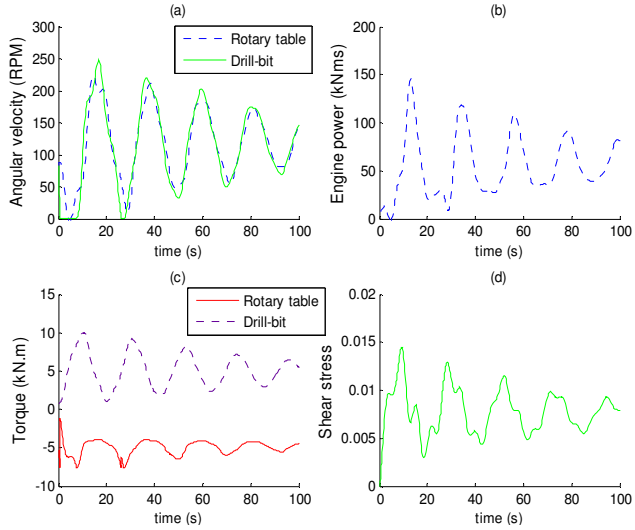

Figure 13 – Time response for 120 kN and 120 rpm with control parameters $k_p = 200$ Nms and $k_i = 100$ Nm.

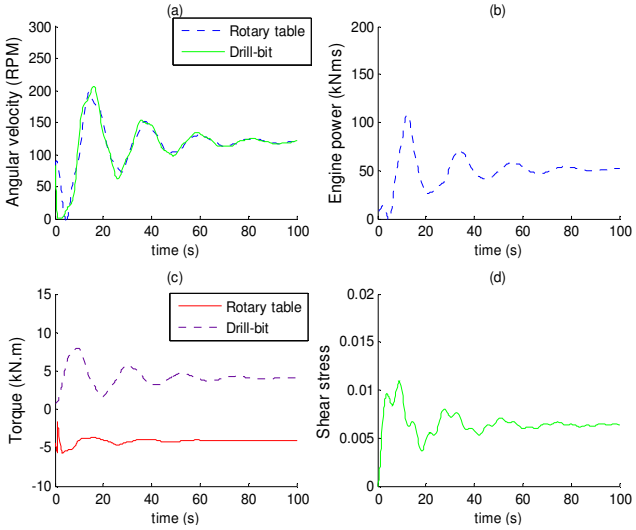

Figure 14 – Time response for 100 kN and 120 rpm with control parameters $k_p = 200$ Nms and $k_i = 100$ Nm.

4.3. Simultaneous variation of control parameters and drilling conditions

The two strategies presented above show to be efficient control techniques. A third strategy would be to combine the first two and simultaneously vary control parameters and drilling conditions. Based on the two previous analyses, it was proposed to improve the reference case, with drilling condition: weight-on-bit 120 kN and drill-bit angular velocity 80 rpm, and control parameters: integral gain k_i 100 Nm and proportional gain k_p 200 Nms, for which the response is shown in Fig. 10, by both moving control parameters to a more effective region and setting the drilling condition to a more favorable one by increasing angular velocity. Figures 15 and 16 shows the time response for drilling conditions with 120 kN and 100 rpm and 120 kN and 120 rpm, respectively, and control parameters k_p 500 Nms and k_i 50 Nm, when compared to the one using only enhanced control parameters (and original drilling condition with 120 kN and 80 rpm). It can be noticed that the simultaneous variation of drilling condition and control parameters may lead to very stable response and, simultaneously, reduce the time the drill-bit remains in the stick phase. The settling time is also a little smaller with lower torque and shear stress values. Only the power required is increased due to the increased target angular velocity. The average rate-of penetration is increased from 15.8 m/h (target 16.3 m/h), for the reference case, to 16.8 m/h (with 100 rpm, target 17.3 m/h) and 17.8 m/h (with 120 rpm, target 18.4 m/h) with optimal control parameters and increasing the target angular velocity.

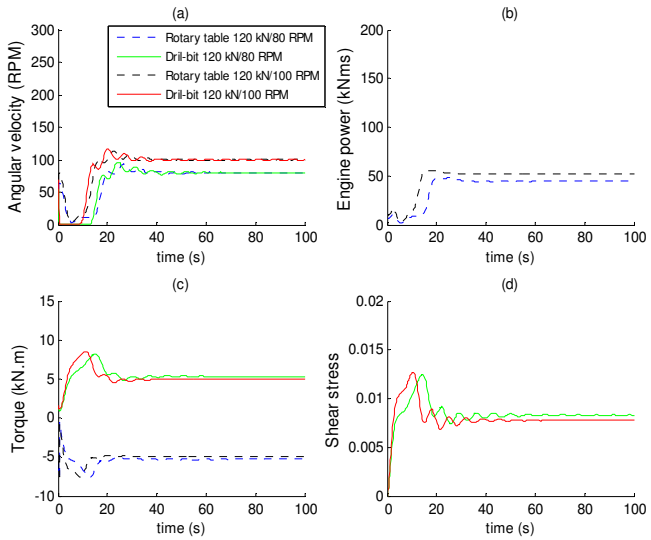

Figure 15 – Time response for 120 kN and 80 rpm (dashed blue and solid green) and 120 kN and 100 rpm (dashed black and solid red) with control parameters $k_p = 500$ Nms and $k_i = 50$ Nm.

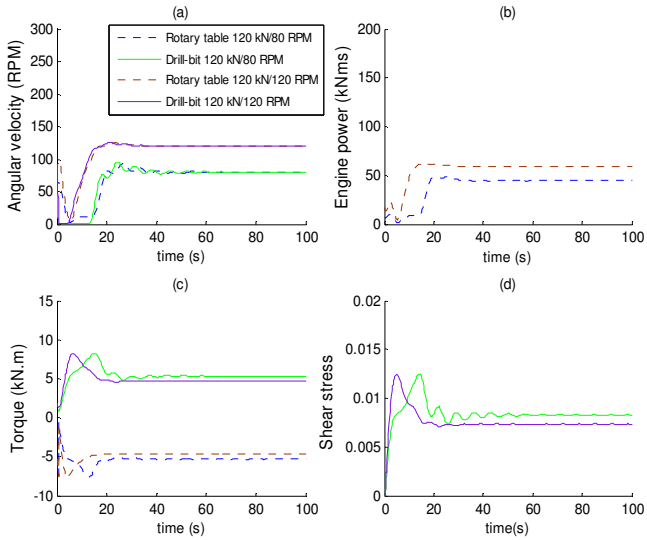

Figure 16 – Time response for 120 kN and 80 rpm (dashed blue and solid green) and 120 kN and 120 rpm (dashed brown and solid purple) with control parameters $k_p = 500$ Nms and $k_i = 50$ Nm.

5. CONCLUSIONS

This work has presented a parametric analysis of the dynamic response of a simplified model for a drilling system composed of driving rotary table, drillstring and bottom-hole-assembly. The drill-bit-formation interaction was modeled using a nonlinear non-regularized dry friction model. The main objective was to show that depending on the operation conditions, weight-on-bit and target angular velocity, there exist well-defined stability regions on the plane formed by the proportional and integral control parameters in which the self-excited torsional vibrations (and oscillatory angular velocities) induced by the stick-slip phenomenon may be reduced. The behaviors of these stability regions in terms of varying operation conditions were analyzed. The effect of the control parameters and operation conditions on some performance and failure criteria, such as average rate-of-penetration, driving torque and power required, maximum drill-bit angular velocity, and maximum shear stress in the drillstring, was also analyzed.

Three strategies were proposed to improve drilling performance: variation of control parameters, variation of drilling conditions and simultaneous variation of control parameters and drilling conditions. It was observed that the three strategies are capable of improving the drilling performance in terms of reducing the number of stick-slip occurrences and its unwanted effects. However, the resulting rate-of-penetration is not significantly affected by the control parameters, but almost only by the drilling conditions. In fact, in some cases, the average rate-of-penetration is even a little higher for unstable conditions (i.e. with persistent stick-slip). Nevertheless, it was shown that proper adjustment of control parameters may allow stable and effective drilling.

6. REFERENCES

Christoforou, A.P. and Yigit A.S., 2003. "Fully coupled vibrations of actively controlled drillstrings". Journal of Sound and Vibration, Vol. 267, pp. 1029-1045.

Elsayed, M.A. and Dareing, D.W. and Vonderheide, M.A., 1997. "Effect of torsion on stability, dynamic forces, and vibration characteristics in drillstring". Journal of Energy Resources Technology, Vol. 119, pp. 11-17.

Jansen, J.D. and van den Steen, L., 1995. "Active damping of self-excited torsional vibration in oil well drillstrings". Journal of Sound and Vibration, Vol. 179, No. 4, pp. 647-668.

Lopez, M.N. and Suarez, R., 2004. "Practical approach to modeling and controlling stick-slip oscilations in oilwell drillstring". Proceedings of the 2004 IEEE International Conference on Control Applications, Taipei, Taiwan, pp. 1454-1460.

Placido, J.C.R., Santos, H.M.R. and Galeano, Y.D., 2002. "Drillstring vibration and wellbore instability". Journal of Energy Resources Technology, Vol. 124, pp. 217-222.

Richard, T. and Detournay, E., 2000. "Stick-slip motion in a friction oscillator with normal and tangential mode coupling". Comptes Rendus de l'Académie des Sciences - Série IIb, Vol .328, pp. 671-678.

Richard, T., Germay, C. and Detournay, E., 2004. "Self-exited stick-slip oscilations of drill bits". Comptes Rendus Mécanique, Vol. 332, No. 8, pp. 619-626.

Ritto, T.G., Soize, C. and Sampaio, R., 2009. "Non-linear dynamics of a drill-string with uncertain model of the bit-rock interaction". International Journal of Non-Linear Mechanics, Vol. 44, pp. 865-876.

Schlumberger Ltd., 2006. "Shock and vibration in the drilling environment". Tutorial video. 8min20s. http://www.slb.com/services/drilling.aspx.

Spanos, P.D., Sengupta, A.K., Cunningham, R.A. and Paslay, P.R., 1995. "Modeling of roller cone bit lift-off dynamics in rotary drilling". Journal of Energy Resources Technology, Vol. 117, pp. 197-207.

Trindade, M.A. and Sampaio, R., 2005. "Active control of coupled axial and torsional drill-string vibrations". Proceedings of 18th COBEM International Congress of Mechanical Engineering, Ouro Preto, MG, in CD-ROM.

Trindade, M.A., Wolter, C. and Sampaio, R., 2005. "Karhunen-Loeve decomposition of coupled axial/bending vibrations of beams subject to impacts". Journal of Sound and Vibration, Vol. 279, pp. 1015-1036.

Tucker, R.W. and Wang, C., 1999a. "On the effective control of torsional vibrations in drilling systems". Journal of Sound and Vibration, Vol. 224, No. 1, pp. 101-122.

Tucker, R.W. and Wang, C., 1999b. "An integrated model for drill-string dynamics". Journal of Sound and Vibration, Vol. 224, No. 1, pp. 123-165.

Tucker, R.W. and Wang, C., 2003. "Torsional vibration control and cosserat dynamics of a drill-rig assembly". Meccanica, Vol. 38, pp. 143-159.

7. RESPONSIBILITY NOTICE

The authors are the only responsible for the printed material included in this paper.